Metal Ir coatings on endocardial electrode tips, obtained by MOCVD

VIKULOVA, Evgeniia S., KAL'NYI, Danila B., SHUBIN, Yury V., KOKOVKIN, Vasily V., MOROZOVA, Natalya B., HASSAN, Aseel <http://orcid.org/0000-0002-7891-8087> and BASOVA, Tamara V.

Published version

VIKULOVA, Evgeniia S., KAL'NYI, Danila B., SHUBIN, Yury V., KOKOVKIN, Vasily V., MOROZOVA, Natalya B., HASSAN, Aseel and BASOVA, Tamara V. (2017). Metal Ir coatings on endocardial electrode tips, obtained by MOCVD. Applied Surface Science, 425, 1052-1058.

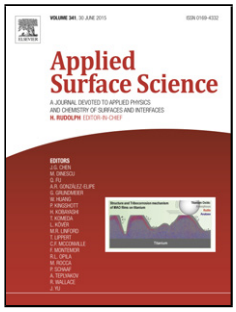

Title: Metal Ir coatings on endocardial electrode tips, obtained by MOCVD

Authors: Evgeniia S. Vikulova, Danila B. Kal'nyi, Yury V. Shubin, Vasily V. Kokovkin, Natalya B. Morozova, Aseel Hassan, Tamara V. Basova

PII: S0169-4332(17)32091-3
DOI: http://dx.doi.org/doi:10.1016/j.apsusc.2017.07.100
Reference: APSUSC 36634

To appear in: *APSUSC*

Received date: 31-3-2017
Revised date: 26-6-2017
Accepted date: 13-7-2017

Please cite this article as: Evgeniia S.Vikulova, Danila B.Kal'nyi, Yury V.Shubin, Vasily V.Kokovkin, Natalya B.Morozova, Aseel Hassan, Tamara V.Basova, Metal Ir coatings on endocardial electrode tips, obtained by MOCVD, Applied Surface Sciencehttp://dx.doi.org/10.1016/j.apsusc.2017.07.100

Metal Ir coatings on endocardial electrode tips, obtained by MOCVD

Evgeniia S. Vikulova[a], Danila B. Kal'nyi[a,b], Yury V. Shubin[a,b], Vasily V. Kokovkin[a,b], Natalya B. Morozova[a], Aseel Hassan[c], Tamara V. Basova[a,b]*

[a]*Nikolaev Institute of Inorganic Chemistry SB RAS, 3 Acad. Lavrentiev Ave., 630090 Novosibirsk, Russian Federation*

[b]*Novosibirsk State University, Pirogova Str. 2, 630090 Novosibirsk, Russian Federation*

[c]*Materials and Engineering Research Institute, Sheffield Hallam University, Sheffield S1 1WB, UK*

* corresponding author:

e-mail: basova@niic.nsc.ru, tel.: +7(383)330-95-56, fax: +7(383)330-94-89

Graphical abstract

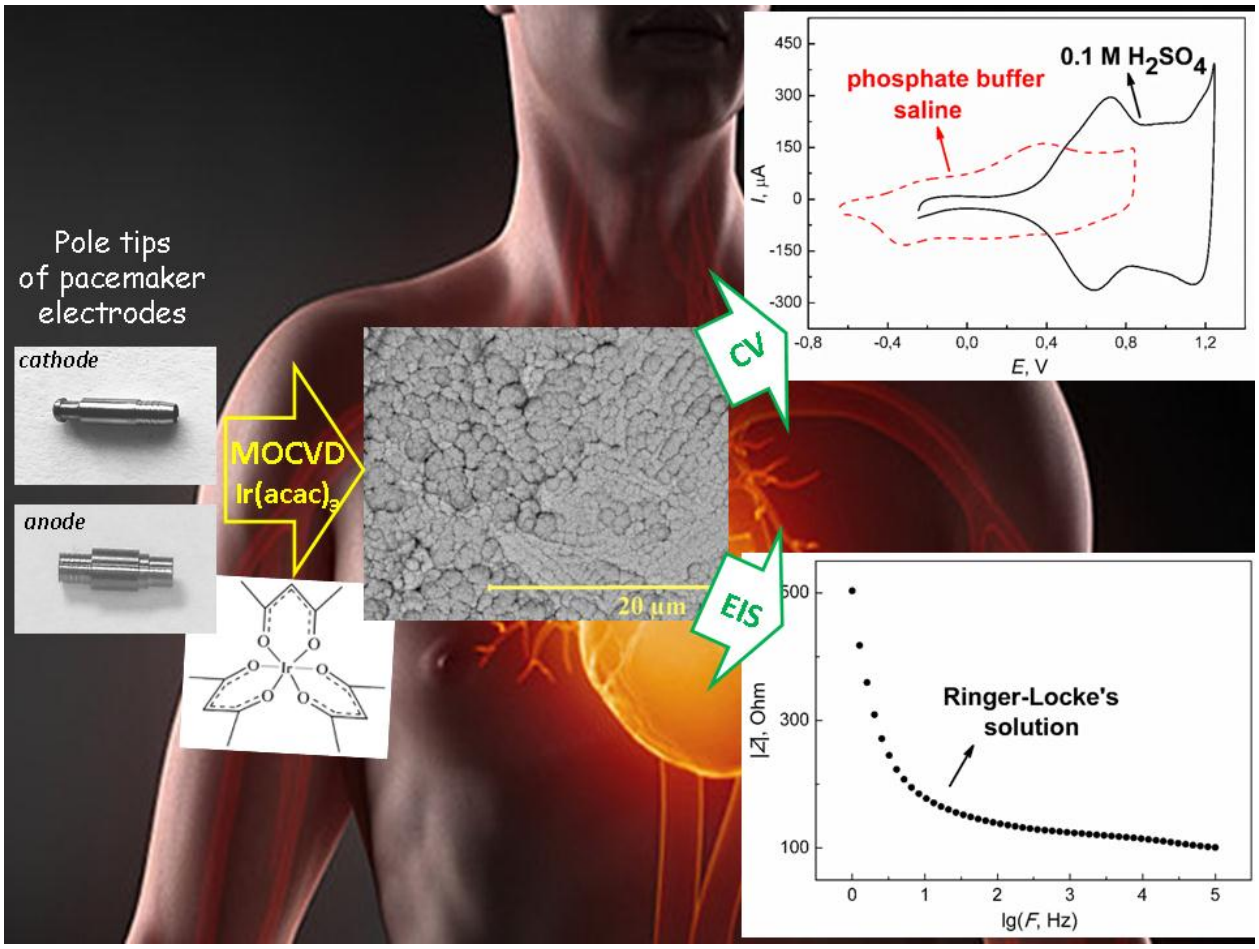

Highlights

- Metal Ir coatings were deposited onto the endocardial electrode tips by MOCVD.
- The formation of coatings with fractal-like morphology was achieved.
- The metal coatings were electrochemically activated in acid media to form AIROFs.
- The AIROF samples obtained are characterized by high capacitance.
- MOCVD is the alternative method for deposition of Ir coatings for medical equipment.

Abstract

The present work demonstrates the application of the Metal-Organic Chemical Vapor Deposition technique to fabricate metal iridium coatings onto the pole tips of endocardial electrodes. Using iridium (III) acetylacetonate as volatile precursor, the target coatings were successfully applied to the working surface of cathodes and anodes of pacemaker electrodes in the flow type reactor in hydrogen atmosphere at deposition temperature of 550°C. The coating samples were characterized by means of XRD, SEM, Raman- and XPS-spectroscopies. The formation of non-textured coatings with fractal-like morphology and 7-24 nm crystallite size has been realized. The electrochemical properties of the coatings were investigated by cyclic voltammetry and electrochemical impedance spectroscopy. The charge storage capacity values of the electrochemically activated samples were 17.0-115 $mC \cdot cm^{-2}$ and 14.4-76.5 $mC \cdot cm^{-2}$ for measurements carried out in 0.1M sulfuric acid and in phosphate buffer saline solutions, respectively. A comparison of some characteristics of the samples obtained with commercially available cathode of pacemaker electrodes is also presented.

Keywords: iridium coating, MOCVD, electrode, pacemaker, charge storage capacity

1. Introduction

Stimulating, recoding, diagnostic and ablating microelectrodes are widely used in modern neuro- and cardiosurgeries. The progress in these important medical fields requires the reduction of the electrodes size and improvement of their performance. The most practical approach to achieve these objectives is through the deposition of functional coatings, which provide the necessary electrochemical characteristics on the electrode working surface that is in direct contact with the tissue. The electrochemical properties of such coatings are determined by the area of the electrode, however the global tendency is to increase capacitive characteristics and reduce the impedance in order to ensure a high charge transfer, improve the signal detection, and decrease the stimulation voltage range and tissue damage [1, 2]. As an example of concrete values, a Helmholtz capacitance of around 5-27 $mF \cdot cm^{-2}$ has recently been patented for implanted cardio pacing electrodes [3-6]. In the case of electrodes applied for neural stimulation the electrode effectiveness could be assessed in terms of one of the estimated electrochemical values, which is the electrode charge storage capacity (CSC) that mostly varied from 0.5 to 220 $mC \cdot cm^{-2}$ [2, 7-9]. Apart from the electrochemical requirements, the electrode coatings must be biocompatible, corrosion resistant, stable to sterilization procedures, and radio-opaque.

The materials employed for electrodes coating are based on noble metals, namely, iridium and platinum. These metals possess all above-mentioned properties together with appropriate electrochemical characteristics making them very effective as coatings of the neuro and cardio microelectrodes [1, 2, 10-13]. Currently a number of methods have been used for the deposition of noble metal materials on the electrodes for medical applications including physical vapor deposition [14, 15], magnetron sputtering [2, 6, 7, 13], electrodeposition [3, 13, 16, 17], chemical bath deposition [18], electron-beam evaporation [19], sol-gel [20], thermal decomposition of the metal salts [5, 13, 21]. Metal Organic Chemical Vapor Deposition (MOCVD) could provide a promising alternative since this method is characterized by a relatively low energy consumption (low deposition temperature of the refractory materials such as iridium and platinum), possibility of the formation of homogeneous coatings on objects that are irregular in shape (including components of medical electrodes) and high precursor utilization factor being especially important in the case of noble metals. MOCVD advantages also include precise multi-parameter control of the coating growth process permitting to

obtain the layers with predetermined composition and microstructure as well as multi-layered or composite coatings in a single experiment and to deposit targeted layers onto the different substrates (metals, semiconductors, non-conductive materials, polymers). However, for the most effective use of the MOCVD method it is necessary to accurately define the experimental conditions based on the thermal properties of the used volatile precursor. Using this approach, we have recently demonstrated a successful application of the MOCVD method for the deposition of platinum onto the pole tips of pacemakers [22, 23]. The formation of iridium-containing coatings on similar objects by MOCVD still presents the unusual challenge that has not been covered in current literature.

This work demonstrates a metal iridium coating onto the cathode pole tips (CPTs) and anode pole tips (APTs) of pacing electrodes (Fig. 1) obtained by the innovative MOCVD method. In order to compare a number of characteristics (electrochemical properties, iridium and impurities content, surface morphology) of the coatings obtained with those of industrial samples the CPT of commercially available iridium electrode (BIOTRONIK SE & Co.KG, PX 60-BP, "iridium fractal" coating, serial number 23543798, catalog number 119 687) was studied.

2. Experimental details

2.1. Deposition of iridium coatings by MOCVD

Iridium(III) acetylacetonate, $Ir(acac)_3$, was used as a volatile precursor. The compound was synthesized according to the procedure developed by Morozova *et al* [24] using iridium powder (99.95%, "Krastsvetmet" JSC, Russia, CAS 7439-88-5) and acetylacetone (99.9%, Dalchem, Russia, CAS 123-54-6) as a metal and ligand sources, respectively. The product was purified by sublimation in vacuum (180°C, $5x10^{-2}$ Torr). Elemental analysis, wt. % (CARLO-ERBA-11008 analyser): for $IrC_{15}O_6H_{21}$ calculated C 36.8, H 4.3, found C 37.0, H 4.4.

The deposition of iridium coatings onto pole tips (PTs) (Co Ltd "Elestim-Kardio", Russia) and onto model substrates (Si(100) plates, 1 x 2 cm^2) were carried out in a vertical flow type cold-wall MOCVD reactor in a reducing atmosphere. Hydrogen with a flow rate $v(H_2)$ 1-2 $l \cdot h^{-1}$ was used as a gas reagent; the deposition time was 2-4 h. The experimental parameters were chosen on the basis of the precursor thermal property data published earlier [25-27]. In particular, the deposition temperature (550°C) was chosen from the data on the thermodecomposition of the precursor's vapor at the heated surface in the presence of hydrogen as the temperature of a maximal decomposition

degree [25]. The evaporator temperature (210°C), total reactor pressure (1 atm) and carrier gas flow rate (Ar, 1-2 $l \cdot h^{-1}$) were selected to provide a partial pressure of the precursor vapor *ca* 1.0 Torr ($\ln P(\text{atm}) = 25.53 - 15557/T(\text{K})$ [26]) and on the basis of investigations of the $Ir(acac)_3$ mass transfer processes [27].

2.2. Coatings characterization

The phase composition of the Ir coatings was studied using a diffractometer Shimadzu XRD-7000 (CuKα-radiation, Ni-filter, angle range 2θ = 25–75°). The crystallite sizes were estimated according to the Scherrer equation [28]. In the case of the coatings deposited onto PTs, special corrections taking into account the contribution of nonplanar sample geometry to the peaks' broadening were used with the initial CPT or APT as references. The surface morphology of all samples and the structure of model samples were studied by scanning electron microscopy (SEM) using JSM-6700F and Hitachi–TM 3000 microscopes. The chemical composition of the coatings on model substrates was determined by X-ray photoelectron spectroscopy (XPS) using Phoibos 150 spectrometer (monochromatic AlKα-radiation, beam diameter *ca* 1 mm). The ion sputtering was made using an IQE 11/35 ion source by Ar^+ ions with energy 1 keV at the ion current density *ca* 7 $\mu A \cdot cm^2$. The energy calibration was performed relative to the surface hydrocarbons C1s peak (285.0 eV). The elemental composition of electrode pole samples was evaluated by energy dispersive X-ray spectroscopy (EDS) using EX-2300BU analyzer; the obtained results are presented in Supplementary Materials (S-1). The Raman spectra (RS) were registered on Triplemate device, SPEX, equipped with a CCD detector in the backscattering geometry using the argon laser (488 nm, 30 mW) for spectrum excitation. The surface roughness of covered and uncovered CPTs was examined by means of atomic force microscopy (AFM) using the SolverP47Bio microscope (NT-MDT, Russia). The examples of the obtained images are shown in Supplementary Materials (S-2). Average roughness (R_a) of selected areas (40x40μm) was obtained using the software of the device:

$$R_a = \frac{1}{N_x \cdot N_y} \sum_{j=1}^{N_y} \sum_{i=1}^{N_x} |Z_{ij} - \mu|$$

(Z_{ij} is the height of point (i,j) and μ is the average height of analysed area). Before this measurement, AFM images were flattened using the second order surface subtraction.

The electrochemical properties of the obtained coatings and CPT "BIOTRONIK" were studied by the methods of cyclic voltammetry (CV) and electrochemical impedance spectroscopy (EIS) using a potentiostat-galvanostat P-30J and impedance meter Z-1500J (Elins, Russia), respectively. The voltammetric and impedance characteristics of the coatings were measured by means of conventional three-electrode cell method. The cell included Ag/AgCl electrode as a reference electrode, platinum grid electrode as a counter electrode and iridium PT as a working electrode.

CV measurements were carried out in solutions of 0.1M H_2SO_4 [29, 30] and phosphate buffer saline (PBS) solution [2, 31] at the sweep rate (ν) of 100 $mV \cdot s^{-1}$. The potentials are given vs. the reference electrode. The values of charge storage capacity in anode semicycle (CSC_A), in cathode semicycle (CSC_C), and total cycle value (CSC) were calculated from the CV-curves as described by Ullah et al [31]. The impedance measurements were performed in Ringer-Locke's solution (the solution composition ($g \cdot l^{-1}$) is 9.00 NaCl, 0.200 KCl, 0.395 $CaCl_2 \cdot 6H_2O$, 0.200 $NaHCO_3$, 1.000 $C_6H_{12}O_6$ (glucose); pH = 7.90) using an excitation sinusoidal signal of 50 mV amplitude in the frequency region of $1–10^5$ Hz at the potential of open circuit. Specific capacitance of the iridium coatings was calculated using geometric surface areas of CPT ($3.5x10^{-2}$ cm^2) and APT ($39x10^{-2}$ cm^2). The characteristics of some samples are presented in Table 1.

Prior to the measurements, the electrodes were electrochemically activated by a procedure similar to that described by Song *et al.* [32] and Lee *et al.* [19, 33] to form activated iridium oxide layers (AIROFs). The cell was filled by 0.1 M sulfuric acid and 50 cycles of working electrode polarization were carried out in the potential range between –0.30 and 1.30 V (vs. Ag/AgCl) at a sweep rate (ν) of 500 mV s^{-1}. After the activation, the electrodes were carefully rinsed by bidistilled water.

3. Results and discussion

3.1. Characterization of metal Ir layers

The deposition conditions for MOCVD experiments were precisely chosen on the basis of the thermal properties of the precursor used to obtain the target metal iridium coatings [25-27]. Since the quantitative study of the composition of coatings on the pole tip (for example, by XPS) is complicated due to the non-planarity and complex shape of these substrates (Figure 1), the planar Si samples obtained from the same MOCVD experiment were used as model objects to complete the coating characterization.

All coatings obtained consist of polycrystalline metal iridium as determined by XRD measurements; typical XRD patterns of the produced coatings are presented in Fig. 2. The crystallite size for coatings deposited on PTs calculated using XRD data varied in the range 7-24 nm while that of corresponding model samples is noticeably smaller (3-12 nm). It should be noted that the increase of the hydrogen flow rate from 1 to 2 $l \cdot h^{-1}$ leads to a twofold growth of the crystallite sizes of coatings deposited onto Si; for example in the [111] direction the value increases from 4.0 to 9.9 nm, whereas in [200] direction it changes from 2.6 to 6.8 nm (deposition time 2 h). In the case of coatings deposited onto Si the estimation of the crystallites size of [111] direction is complicated by overlapping of the Ir and substrate peaks (Fig. 2), while the sizes of crystallites in [200] and [220] directions remain practically the same at different $v(H_2)$. At the same time, the ratio of the intensities of iridium (111) and (200) reflections in the diffraction patterns of coatings obtained both on Si and PTs in the same experiment is almost equal (*ca* 2:1) indicating the absence of texture in both cases in the whole deposition parameters interval.

Raman spectra of the coatings on both types of substrates (Si and PT) do not contain any visible peaks corresponding to carbon and are similar to that of the powder metal iridium (JSC "Krastsvetmet", Russia, 99.97%) studied as a standard (Fig. 3). The obtained data show the absence of noticeable amounts of free carbon in the deposited Ir coatings.

The XPS investigations of coatings on Si substrates confirm the results obtained by other methods: the iridium presents only in the form of Ir^0 throughout the etching depth (binding energy of $Ir4f_{5/2}$ and $Ir4f_{7/2}$ are 63.8 eV and 60.8 eV, respectively [34-36]). The typical XPS spectrum is presented in Fig. 4 for the coating obtained at $v(H_2) = 2\ l \cdot h^{-1}$ and deposition time 2 h. As impurities, the iridium layer contains 4 at. % of carbon and 11-12 at. % of oxygen (O/Ir ratio is approximately 0.15), which may be assumed to be carbon-containing by-products generated from the organic ligand during precursor decomposition and included into the coating due to its high growth rate [37].

According to SEM data, the whole coverage of the PT working surface has been achieved in all MOCVD experiments. It should be noted that fractal or fractal-like morphology of noble metal coating are preferable for medical applications [38]. The coatings with surfaces consisted of spherical fractal-like agglomerates ~0.5-2 μm in diameter have been shown to form in the interval of deposition parameters used in this work (Fig. 5a). According to AFM investigation, the average roughness of the samples

deposited onto CPTs varies from 182 to 298 nm rising with increasing hydrogen flow rate and deposition time.

The microstructure and thickness of the Ir coatings have been investigated by SEM measurements carried out for the cross-sections of model planar samples; Typical SEM images are presented in Fig. 6. The thickness of the obtained coatings varied in the range 0.31-1.67 μm. It has been shown that the increase of hydrogen flow rate or deposition time in the used MOCVD parameters interval leads to the near linear growth of the iridium layer thickness while no significant changes are observed in the column coating microstructure (Table 1). For example, the thickness of coatings deposited at a constant hydrogen flow rate (2 $l \cdot h^{-1}$) and varying deposition times 2 and 4 h are 0.78 μm and 1.67 μm, respectively (Fig. 6). These observations are generally consistent with the literature data [39]. However, it should be noted that the coating growth rate on Si and PT seems to be noticeably different, as was indicated by the distinct morphologies and crystallite size for samples obtained in the same MOCVD experiment. One of the possible reasons of this observation seems to be the different nature of the substrates causing diverse adsorption of the precursor vapors and, therefore, various mechanisms for the coating growth [40]. A different morphology of substrates could also play an important role in the growth process: in the case of electrode poles, noticeable defects may contribute to the growth of fractal agglomerates.

A comparison of the deposited samples with the commercial CPT "BIOTRONIK" shows that the surface morphology of these objects differs substantially; in the case of MOCVD more continuous coatings characterized by the absence of visible pores are formed (Fig. 5). It was shown by means of XRD that the coating of CPT "BIOTRONIK" is also characterized by non-textured metal iridium (Fig. 2), however the crystallite size in this case is rather larger (25-35 nm). The comparative estimation of the elemental composition (EDX data) of the studied sample indicates 2-3.3 times higher content of iridium in the coatings obtained in the present work. Furthermore, in contrast to the samples obtained in this work there are two peaks at 1440 and 1610 cm^{-1} ascribed to amorphous carbon in the Raman spectra of CPT "BIOTRONIK" (Fig. 3).

3.2. Electrochemical properties of activated Ir layers

In addition to direct application of Ir electrodes, one of the promising directions for the utilization of the metallic iridium films is their electrochemical activation to produce activated iridium oxide films (AIROFs) [41-47]. AIROF-coated electrodes are

characterized by significantly lower impedance which is important both for cardiac pacing [1, 42, 47-49] and for neurostimulation [2, 43, 44-46]. Following to this trend, in the present work we performed the oxidizing electrochemical activation of the obtained metal samples in a sulfuric acid medium.

The changes in the CV curves during activation are shown in Supplementary materials (S-3) and correspond to the classical growth of the hydrated oxidized iridium multilayers [50-52]. In particular, there are no cathode and anode peaks at 0.60-0.80V (reversible transition Ir(III) → Ir(IV)) on the CV curves of the samples before activation (as-deposited Ir samples), whereas these peaks increase with the number of activation cycles. It is necessary to mention that there were no noticeable changes on XRD patterns and EDS spectra of the samples before and after activation, indicating that the hydrated iridium oxide layer formed during the activation appears to be rather thin and amorphous. Nevertheless, the average roughness of the activated samples was 1.1-1.3 times higher than that of as-deposited ones; the example of surface morphology of Ir(c)-4 sample is given in Supplementary materials (S-2) as an example. The scotch tape tests carried out similarly to Hssein *et al* [53] of as-deposited and activated samples confirmed the high adhesion of the coating to the CPT substrates.

CV curves for the electrodes (sample Ir(c)-4) after the activation procedure are presented in Fig. 7a as an example. The curve profiles are typical for those of oxidizing polycrystalline iridium [19, 33, 50-52]. The characteristic feature is the main cathode and anode peaks in the potential range of 0.60-0.80 V attributed to the reversible redox transformation Ir(IV)/Ir(III). The ratios of CSC_A/CSC_C are close to 1 (0.92-1.01), exhibiting the reversibility of electron transfer processes taking place on the electrode. The values of full cycle CSC of the coatings vary in the range of 17.0-115 $mC \cdot cm^{-2}$. The capacity values increase with increasing of the coatings' thickness and roughness (Table 1). In the case of PBS solutions, the expected peaks shift in the cathodic direction (0.4V) occurs due to the differences in pH of the solutions (Fig. 6a). At the same time the CSC values decrease slightly (14.4-76.5 $mC \cdot cm^{-2}$); nevertheless, the CSC_A/CSC_C ratio remains close to unity (0.93-0.98).

It should be noted that the oxidizing electrochemical activation of the metal iridium coatings formed by MOCVD is more effective than that of the electron-beam evaporated samples: only 9.7 $mC \cdot cm^{-2}$ CSC values of AIROFs in physiological saline solution (100 $mV \cdot s^{-1}$) have been achieved in the last case after 1000 activation cycles in 0.1M H_2SO_4 [19]. Also, the CSC values of the samples obtained in the present work are

noticeably higher than the typical values given in the literature for AIROF electrodes formed from iridium wire and sputtered iridium during other activation procedures: 4.4-40.3 $mC \cdot cm^{-2}$ (in PBS or physiological solution, 100 $mV \cdot s^{-1}$) [46]. Therefore MOCVD seems to be promising as a "first-step method" to obtain AIROFs probably because in this case metal iridium coating with more developed surface are formed.

To compare the data, the CPT "BIOTRONIK" was also electrochemically activated under the same conditions. After such activation the shapes of CV curves of CPT "BIOTRONIK" are similar to those of MOCVD coatings (Fig. 7a); CSC_A/CSC_C ratios in both electrolytes are also close to 1 (0.97-1.01). The calculated CSC values for CPT "BIOTRONIK" are 117 $mC \cdot cm^{-2}$ in sulfuric acid and 95.1 $mC \cdot cm^{-2}$ in PBS solution and are comparable with the maximal CSC characteristics of the coatings obtained in this work.

The impedance spectra and phase angle spectra of the samples obtained and CPT "BIOTRONIK" are similar to those of AIROF electrodes [45] (Fig. 7b). Within the frequency range 10^2–10^5 Hz, the impedance amplitude and phase angle are nearly independent of frequency and show resistive behavior. The values of the resistance component of the impedance are 123 Ω and 50-150 Ω for CPT "BIOTRONIK" and the samples obtained in this work, respectively. Both impedance amplitude and phase angles become frequency dependent at frequencies below 100 Hz. The specific capacity value estimated from the spectra at the frequency 1 Hz for CPT "BIOTRONIK" is 5.4 $mF \cdot cm^{-2}$ while in the case of MOCVD coatings these values vary in the range 0.63-10.0 $mF \cdot cm^{-2}$, i.e. the specific capacity values of the samples obtained are also comparable with those for the commercial electrode.

4. Conclusions

The work describes the first example of deposition of metal Ir coatings onto the electrode poles of pacemaker electrodes by MOCVD method. The samples obtained were characterized by means of XRD, SEM, Raman- and XPS-spectroscopy to provide clear evidence of the formation of non-textured metal Ir coatings with fractal-like morphology and relatively low carbon impurities content. The obtained samples could be effectively used as the basis for simple producing of AIROF as it has been demonstrated by cyclic voltammetry and electrochemical impedance spectroscopy of the activated coatings. The AIROF samples were shown to possess high charge storage capacity values: 17.0-115 $mC \cdot cm^{-2}$ (0.1M sulfur acid) and 14.4-76.5 $mC \cdot cm^{-2}$

(phosphate buffer saline). The electrochemical characteristics of the obtained coatings are close to those of commercially available cathodes.

The results obtained here demonstrate the prospects of a MOCVD technique for deposition of Ir-containing coatings on the working surfaces of electrodes as a key step for miniaturization and efficiency increase of the apparatus for high-tech cardio- and neurosurgery.

Acknowledgments

E. S. Vikulova is grateful to the Council on the Grants from the President of the Russian Federation (SP-3215.2016.4) for financial support. The authors thank PhD E. A. Maksimovsky (NIIC SB RAS) for the SEM-EDS investigation.

References

[1] M. Schaldach, Electrotherapy of the Heart, Springer-verlag, Berlin, 1992.

[2] S.F. Cogan, Neural stimulation and recording electrodes, Annu. Rev. Biomed. Eng. 10 (2008) 275-309.

[3] D.M. Zhou, Platinum electrode surface coating and method for manufacturing the same, US 7887681 B2, 2011.

[4] O. Keitel, F. Krüger, M. Ponitz, Selective parylene coating for cardiac pacemaker electrodes, US 20090312825 A1, 2009.

[5] L. Atanasoska, R.W. Heil, D.M. Flynn, Coatings for implantable electrodes, US 8017178 B2, 2011.

[6] F. Krüger, H. Specht, H.-J. Wachter, O. Keitel, Stimulation electrode with porous coating, US 7603169 B2, 2009.

[7] S. Negi, R. Bhandari, L. Rieth, F.Solzbacher, In vitro comparison of sputtered iridium oxide and platinum-coated neural implantable microelectrode arrays, Biomed. Mater., 5 (2010), 015007 and references therein

[8] X. Luo, C.L. Weaver, D.D. Zhou, R. Greenberg, X. T. Cui, Highly stable carbon nanotube doped poly(3,4-ethylenedioxythiophene) for chronic neural stimulation, Biomaterials 32 (2011) 5551-5557.

[9] E. Pérez, M.P. Lichtenstein, C. Suñol, N. Casañ-Pastor, Coatings of nanostructured pristine graphene-IrOx hybrids for neural electrodes: Layered stacking and the role of non-oxygenated grapheme, Mater. Sci. Eng. C 55 (2015) 218-226.

[10] L.A. Geddes, R. Roeder, Criteria for the selection of materials for implanted electrodes. Annals of biomedical engineering, Ann. Biomed. Eng. 31, (2003) 879-890.

[11] A. Cowley, A healthy future: platinum in medical applications, Platinum Metals Rev. 55 (2011) 98-107.

[12] T.D. Kozai, N.A. Alba, H. Zhang, N.A. Kotov, R.A. Gaunt, X.T. Cui, Nanotechnology and neuroscience: nano-electronic, photonic and mechanical neuronal interfacing, in: M. De Vittorio, L. Martiradonna, J. Assad (Eds.) Nanotechnology and Neuroscience: Nano-electronic, Photonic and Mechanical Neuronal Interfacing, Springer-Verlag, New York, 2014, pp 71-134.

[13] N.P. Aryan, H. Kaim, A. Rothermel, Stimulation and Recording Electrodes for Neural Prostheses, Springer International Publishing, New York, 2015.

[14] H. Specht, F. Krueger, HJ Wachter, O. Keitel, C. Leitold, M. Frericks, Electrochemical properties and stability of PVD coatings for the application in cardiac

and neurological stimulation, Med. Device Mater. III, Proc. 3rd Mater. Processes Med. Devices Conf., 2006, 169.

[15] L. Atanasoska, P. Gupta, C. Deng, R. Warner, S. Larson, J. Thompson, XPS, AES, and electrochemical study of iridium oxide coating materials for cardiovascular stent application. ECS Trans. 16 (2009) 37-48.

[16] C.R.K. Rao, D.C. Trivedi, Chemical and electrochemical depositions of platinum group metals and their applications Coord. Chem. Rev. 249 (2005) 613-631.

[17] A. Petrossians, J.J. Whalen, J.D. Weiland, F. Mansfeld, Electrodeposition and characterization of thin-film platinum-iridium alloys for biological interfaces, J. Electrochem. Soc. 158 (2011) D269-D276.

[18] Y.M. Chen, T.W. Chung, P.W. Wu, P.C. Chen, A cost-effective fabrication of iridium oxide films as biocompatible electrostimulation electrodes for neural interface applications, J. Alloy Compd. 692 (2017) 339-345.

[19] I.S. Lee, C.N. Whang, K. Choi, M.S. Choo, Y.H. Lee, Characterization of iridium film as a stimulating neural electrode, Biomaterials 23 (2002) 2375-2380.

[20] C.M. Nguyen, S. Rao, X. Yang, S. Dubey, J. Mays, H. Cao, J.C. Chiao, Sol-Gel Deposition of Iridium Oxide for Biomedical Micro-Devices, Sensors 15 (2015) 4212-4228.

[21] S. Musić, S. Popović, M. Maljković, Z. Skoko, K. Furić, A. Gajović, Thermochemical formation of IrO_2 and Ir, Mater. Lett. 57 (2003) 4509-4514.

[22] N.V. Gelfond, V.V. Krisyk, S.I. Dorovskikh, D.B. Kal'nyi, E.A. Maksimovskii, Y.V. Shubin, S.V. Trubin, N.B. Morozova, Structure of platinum coatings obtained by chemical vapor deposition, J. Struct. Chem. 56 (2015) 1215-1219.

[23] S.I. Dorovskikh, G.I. Zharkova, A.E. Turgambaeva, V.V. Krisyuk, N.B. Morozova, Chemical vapour deposition of platinum films on electrodes for pacemakers: Novel precursors and their thermal properties, Appl. Organomet. Chem. 31 (2017) AOC3654, doi:0.1002/aoc.3654.

[24] I.K. Igumenov, V.G. Isakova, N.B. Morozova, V.A. Shipachev, The method of preparation of rare metal tris-β-diketonates, EAN Pat. 000402, 1999.

[25] N.V. Gelfond, N.B. Morozova, P.P. Semyannikov, S.V. Trubin, I.K. Igumenov, A.K. Gutakovskii, A.V. Latyshev, Preparation of thin films of platinum group metals by pulsed MOCVD. I. Deposition of Ir layers, J. Struct. Chem. 53 (2012) 715-724.

[26] N.B. Morozova, P.P. Semyannikov, S.V. Sysoev, V.M. Grankin, I. K. Igumenov, Saturated vapor pressure of iridium (III) acetylacetonate, J. Therm. Anal. Calorim. 60 (2000) 489-495.

[27] N.V. Gelfond, A.N. Mikheev, N.B. Morozova, N.E. Gelfond, I.K. Igumenov, Experiment and modeling of mass-transfer processes of volatile metal beta-diketonates. II. Study of mass-transfer process of tris-(acetylacetonato)iridium (III), Int. J. Therm. Sci. 42 (2003) 725-730.

[28] B.D. Cullity, Elements of X-ray Diffraction, Addison-Wesley Publishing Company, Reading, Massachusetts, USA, 1978.

[29] Capon, R. Parsons, The effect of strong acid on the reactions of hydrogen and oxygen on the noble metals. A study using cyclic voltammetry and a new teflon electrode holder, J. Electroanal. Chem. 39 (1972) 275-286.

[30] J.M.D. Rodríguez, J.A.H. Melián, J.P. Peña, Determination of the real surface area of Pt electrodes by hydrogen adsorption using cyclic voltammetry, J. Chem. Educ. 77 (2000) 1195-1197.

[31] N. Ullah, S. Omanovic, Large charge-storage-capacity iridium/ruthenium oxide coatings as promising material for neural stimulating electrodes, Mater. Chem. Phys. 159 (2015) 119-127.

[32] I. Song, K. Fink, J.H. Payer, Metal oxide/metal pH sensor: Effect of anions on pH measurements, Corrosion, 54 (1998) 13-19.

[33] I.S. Lee, C.N. Whang, Y.H. Lee, G.H. Lee, B.J. Park, J.C. Park, W.S. Seo, F.Z. Cui, Formation of nano iridium oxide: material properties and neural cell culture, Thin Solid Films 475 (2005) 332-336.

[34] NIST X-ray Photoelectron Spectroscopy Database, Version 4.1 (National Institute of Standards and Technology, Gaithersburg, 2012); http://srdata.nist.gov/xps/.

[35] B. Wessling, W. Mokwa, U. Schnakenberg, RF-sputtering of iridium oxide to be used as stimulation material in functional medical implants, J. Micromech. Microeng. 16 (2006) S142-S148.

[36] N.V. Gelfond, I.K. Igumenov, A.I. Boronin, V.I. Bukhtiyarov, M.Y. Smirnov, I.P. Prosvirin, R. I. Kwon, An XPS study of the composition of iridium films obtained by MO CVD, Surf. Sci. 275 (1992) 323-331.

[37] I.K. Igumenov, N.V. Gelfond, N.B. Morozova, H. Nizard, Overview of coating growth mechanisms in MOCVD processes as observed in Pt group metals, Chem. Vapor Depos. 13 (2007) 633-637.

[38] M. Schaldach, Fractal coated leads: Advanced surface technology for genuine sensing and pacing, Prog. Biomed. Res. 5 (2000) 259-272.

[39] N.V. Gelfond, N.B. Morozova, I.K. Igumenov, E.S. Filatov, S.A. Gromilov, R.I. Kvon, Structure of Ir-Al_2O_3 coatings obtained by chemical vapor deposition in the hydrogen atmosphere, J. Struct. Chem. 50 (2009) 919-922.

[40] Y.M. Sun, J.P. Endle, K. Smith, S. Whaley, R. Mahaffy, J.G. Ekerdt, J.M. White, R.L. Hance, Iridium film growth with indium tris-acetylacetonate: oxygen and substrate effects. Thin Solid Films, 346 (1999) 100-107.

[41] L.S. Robblee, J.L. Lefko, S.B. Brummer, Activated Ir: An electrode suitable for reversible charge injection in saline solution, J. Electrochem. Soc. 130 (1983)731-733.

[42] J. Riedmüller, A. Bolz, H. Rebling, M. Schaldach, Improvement of stimulation and sensing performance of bipolar pacemaker leads, Conf. Proc. IEEE Eng. Med. Biol. Soc. 6 (1992) 2364-2365.

[43] G.E. Loeb, R.A. Peck, J. Martyniuk, Toward the ultimate metal microelectrode. J. Neurosci. Meth., 63 (1995) 175-183.

[44] S.F. Cogan, P.R. Troyk, J. Ehrlich, T.D. Plante, D.E. Detlefsen, Potential-biased, asymmetric waveforms for charge-injection with activated iridium oxide (AIROF) neural stimulation electrodes, IEEE Trans. Biomed. Eng. 53 (2006) 327–332.

[45] Y. Lu, Z. Cai, Y. Cao, H. Yang, Y.Y. Duan, Activated iridium oxide films fabricated by asymmetric pulses for electrical neural microstimulation and recording, Electrochem. Comm. 10 (2008) 778–782.

[46] X. Kang, J. Liu, H. Tian, C. Zhang, B. Yang, Y. NuLi, H. Zhu, C. Yang, Controlled activation of iridium film for AIROF microelectrodes, Sens. Actuators B Chem. 190 (2014) 601-611.

[47] G. Sallee, K.L. Gunter, D. Frankson, P.A. Merriam, E.J. Maierhofer, M.P. Jones, Flexible electrode for cardiac sensing and method for making, US 20170049349 A1, 2016.

[48] A.G. Bufalo, J. Schaepfer, M. Fromer, L. Kappenberger,. Acute and Long-Term Ventricular Stimulation Thresholds with a New, Iridium Oxide-Coated Electrode, Pacing Clin. Electrophysiol. 16 (1993) 1240-1245.

[49] M.J. Niebauer, B. Wilkoff, Y. Yamanouchi, T. Mazgalev, K. Mowrey, P. Tchou, Iridium oxide–coated defibrillation electrode, Circulation 96 (1997) 3732-3736.

[50] J. Mozota, B.E. Conway, Surface and bulk processes at oxidized iridium electrodes—I. Monolayer stage and transition to reversible multilayer oxide film behaviour, Electrochim. Acta 28 (1983) 1-8.

[51] V. Birss, R. Myers, H. Angerstein-Kozlowska, B.E. Conway, Electron microscopy study of formation of thick oxide films on Ir and Ru electrodes, J. Electrochem. Soc. 131 (1984) 1502-1510.

[52] P.G. Pickup, V.I. Birss, A model for anodic hydrous oxide growth at iridium, J. Electroanal. Chem. Interfacial Clectrochem. 220 (1987) 83-100.

[53] M. Hssein, S. Tuo, S. Benayoun, L. Cattin, M. Morsli, Y. Mouchaal, M. Addou, A. Khelil, J.C. Bernède. Cu-Ag bi-layer films in dielectric/metal/dielectric transparent electrodes as ITO free electrode in organic photovoltaic devices, Org. Electron. 42 (2017) 173-180.

Figure captions

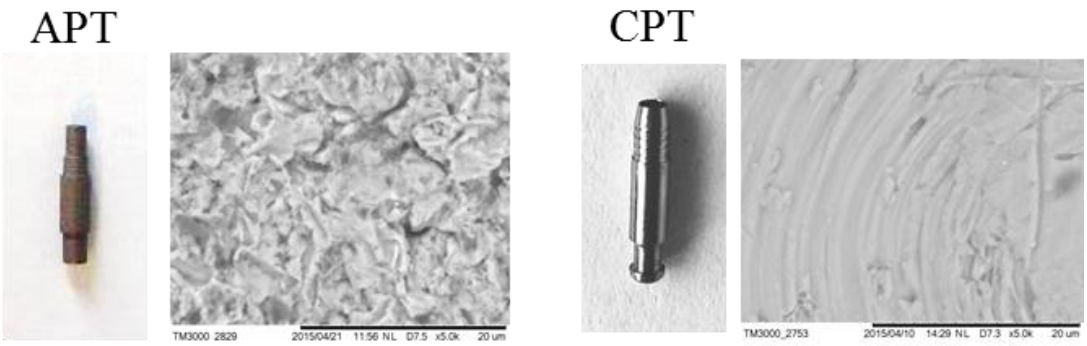

Figure 1. Images of initial anode pole (APT) tip and cathode pole tip (CPT) and their working surfaces.

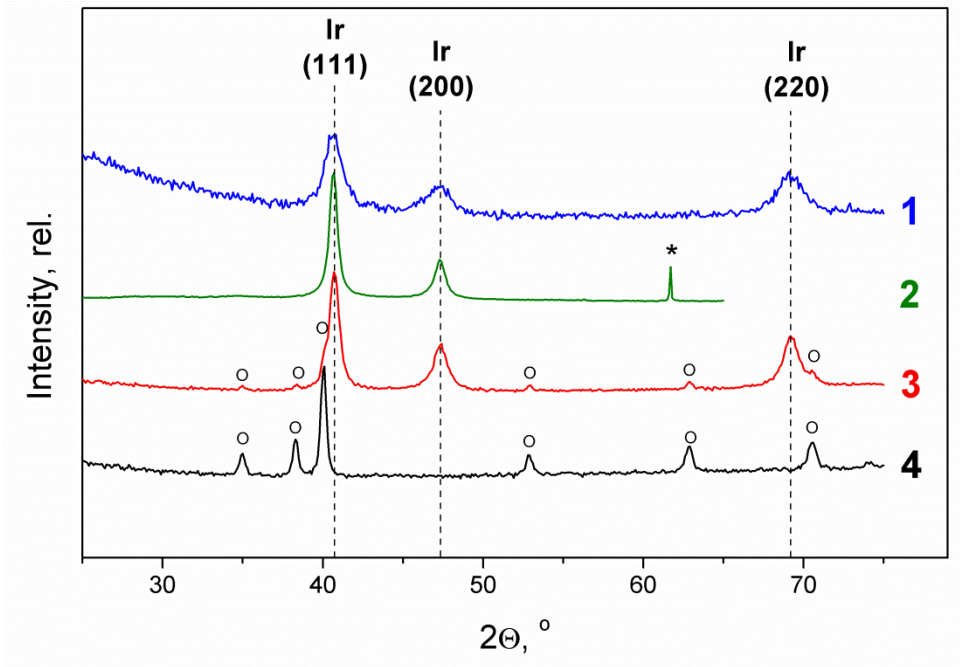

Figure 2. Typical X-ray diffraction patterns of iridium coatings deposited onto Si(100) (**2**) and APTs (**3**) in the same experiments in comparison with diffraction patterns of uncovered APT (**4**) and CPT "BIOTRONIK" (**1**). The circles (○) denote the

reflexes related to the titanium phase of APT, the asterisk (*) designates the $K_\beta(400)$ silicon reflex.

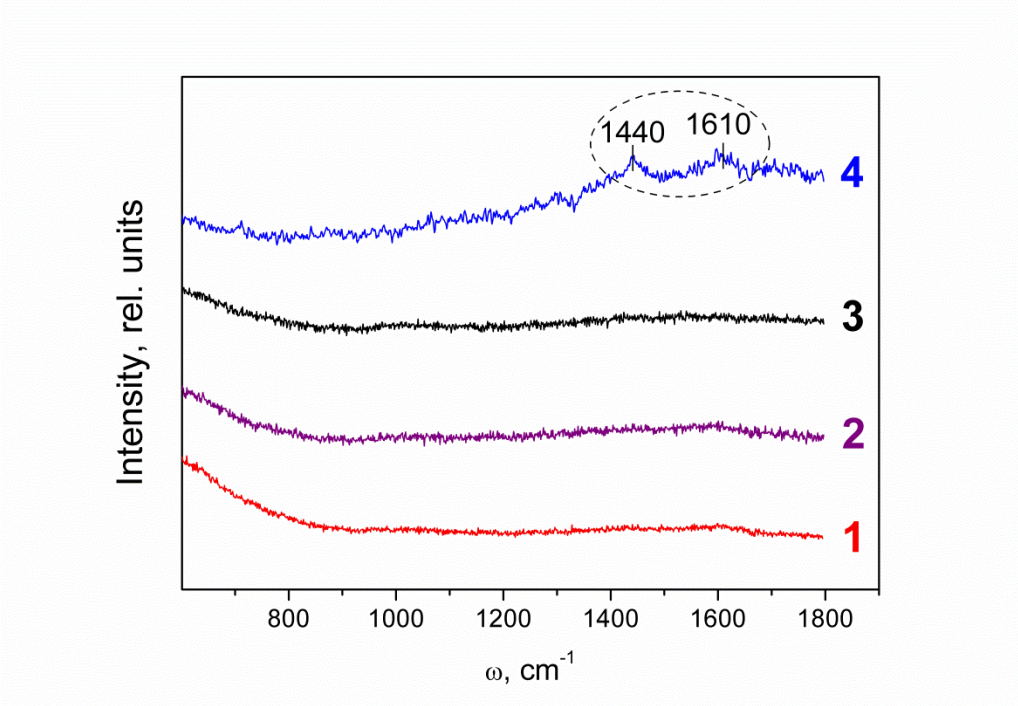

Figure 3. Typical Raman spectra of iridium coatings on CPT (**1**), on Si (**2**), metal Ir powder (**3**) and CPT "BIOTRONIK" (**4**).

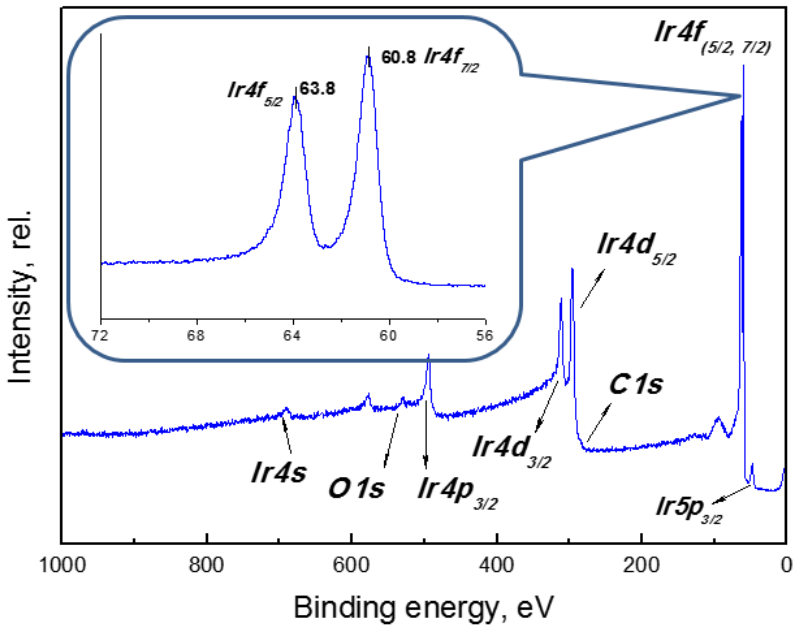

Figure 4. XPS survey spectrum of metal Ir coating on Si substrate after 5 min of Ar^+ etching.

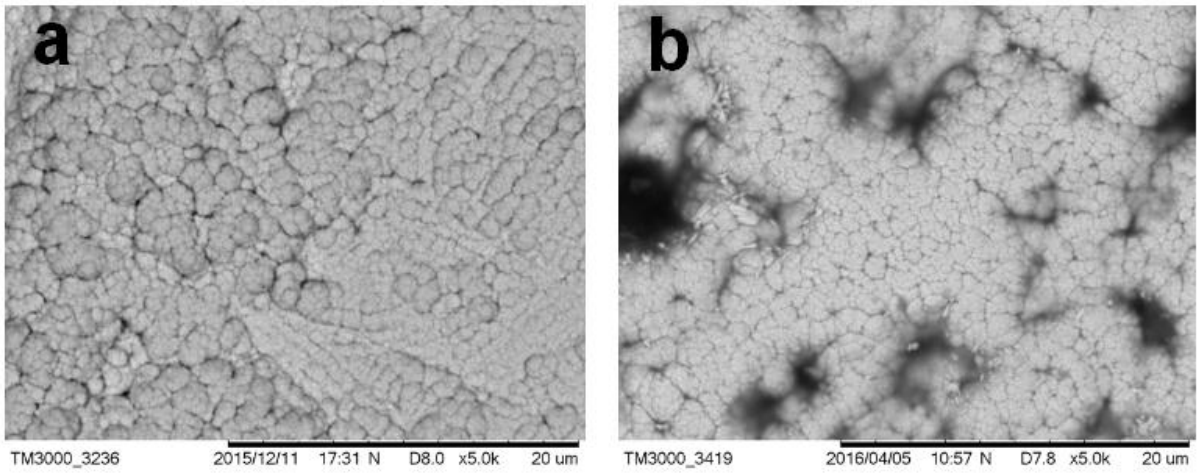

Figure 5. SEM images of Ir(c)-4 sample (a) and CPT "BIOTRONIK" (b).

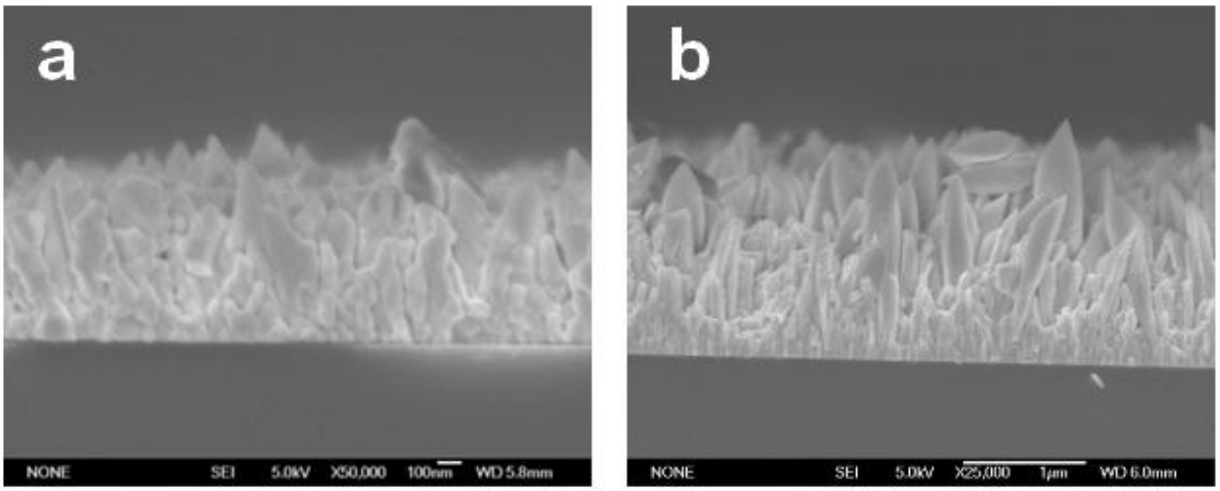

Figure 6. SEM images of a cross-section of the Ir coating deposited onto Si at $v(H_2) = 2\ l \cdot h^{-1}$ and deposition time 2 h (*a*) and 4 h (*b*) (Ir(c)-3 and Ir(c)-4 samples, respectively).

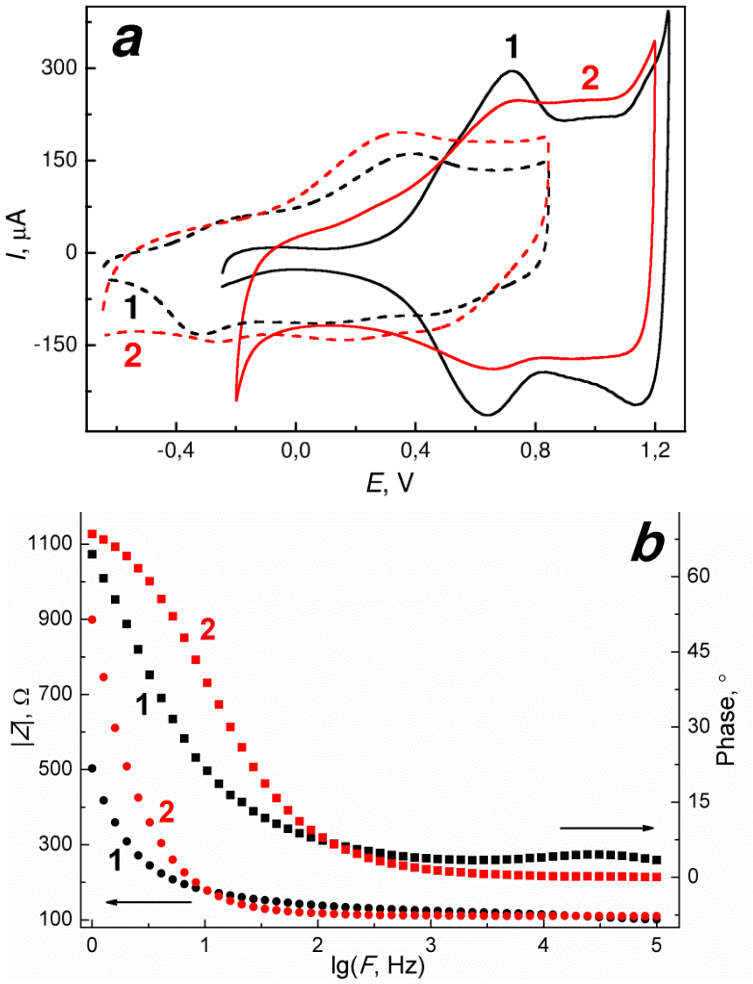

Figure 7. Electrochemical characteristics of activated Ir(c)-4 sample (**1**) and CPT "BIOTRONIK" (**2**): (*a*) CV curves in 0.1M H_2SO_4 (solid lines) and PBS solution (dash lines), (*b*) impedance amplitude (circles) and phase angle (squares) spectra in Ringer-Locke's solution.

Table 1. Deposition conditions and the characteristics of the selected coatings obtained onto the electrode poles.

Sample	Pole	v(H_2), $l \cdot h^{-1}$	Deposition time, h	Thickness (on Si), μm	R_a*, nm	CSC*, $mC \cdot cm^{-2}$					
						0.1 M H_2SO_4			PBS		
						CSC_C	CSC_A	Full	CSC_C	CSC_A	Full
Ir(c)-1	CPT	1	2	0.31	214	8.8	8.2	17.0	7.0	7.4	14.4
Ir(a)-2	APT	1	3	0.50	-	27.8	28.8	56.6	19.1	17.8	36.9
Ir(c)-3	CPT	2	2	0.78	303	39.2	39.0	78.2	28.5	26.8	55.3
Ir(a)-4	APT	2	4	1.67	-	56.4	58.6	115	31.9	30.9	62.8
Ir(c)-4	CPT				327	57.4	57.3	114.7	38.7	37.8	76.5

* activated samples; average roughness of uncovered CPT and CPT “Biotronic” is 188 nm and 352 nm, respectively